Heat treatment of calcium alginate films obtained by ultrasonic atomizing: physicochemical characterization

Marina Soazo[a,b], Germán Báez[a,b], Andrea Barboza[b], Pablo A. Busti[b], Amelia Rubiolo[c], Roxana Verdini[a,b], Néstor J. Delorenzi[b]*

[a]Instituto de Química Rosario (UNR-CONICET), Suipacha 570, 2000 Rosario, Argentina

[b]Facultad de Ciencias Bioquímicas y Farmacéuticas, Universidad Nacional de Rosario, Suipacha 531, 2000 Rosario, Argentina

[c]Instituto de Desarrollo Tecnológico para la Industria Química (UNL-CONICET), Güemes 3450, 3000, Santa Fe, Argentina

* Corresponding author. Tel/Fax: 54-341-4804598

E-mail address: ndeloren@fbioyf.unr.edu.ar

Abtract

Planar films of calcium alginate were obtained using an ultrasonic atomizing device. Sodium alginate solutions of 0.6% and 0.9% (w/v) were nebulized with calcium gluconolactate solutions (gelling agent) of 0, 1, 2 and 3% (w/v) at a flow rate of 0.3 mL min□1 for 20 min. After drying, thickness and mechanical properties were determined. In view of the results of mechanical properties, manageability and flexibility, calcium alginate films obtained using 0.9% sodium alginate and 2% calcium gluconolactate were selected as "optimum dry film" samples. These samples were cut into rectangular pieces and heated at 180°C for 0, 4, 8, 12, 20 and 24 min. Thickness, mechanical and optical properties, differential scanning calorimetry (DSC) thermograms, Fourier transform infrared spectroscopy (FTIR) spectra, and scanning electron microscopy (SEM) micrographs were analyzed in order to characterize the physicochemical properties of heat-treated samples. The heat treatment produced thickness reduction, a yellow ochre color development and an increase in the brittleness of the films. DSC, FTIR and SEM studies suggested that heat treatment produced further dehydration of dry films and thermal dehydration-degradation of alginate macromolecules.

Key words: Calcium alginate films, Ultrasonic atomizing, Heat treatment, Physicochemical characterization

1. Introduction

Sodium alginate is one of the most important polysaccharides used for hydrogels preparation (Draget, 2000). The hydrogel properties are typically controlled by alginate chemical microstructure determined by α-L-guluronic and β-D-mannuronic present in varying proportions and sequences, type of gelling ions and gelling conditions. Alginate gelation occurs when divalent cations (usually Ca^{2+}) interact with blocks of guluronic residues. According to the "egg-box" model (Grant, Morris, Rees, & Smith, 1973), two contiguous, diaxially linked guluronic residues form a cavity that acts as a binding site for calcium ions. This binding induces chain-chain associations forming stable junction zones of dimers and lateral interactions between these dimers. As a result, the gel is formed and mechanical properties are directly related to the number of "egg-box" sites. Thus, the increase in network crosslink density results in a higher fracture stress.

The procedure of introducing gelling ions is an additional parameter influencing the properties of alginate hydrogels (Draget, 2000). The external gelling method consists in exposing alginate solution directly to the gelling ions solution and alginate hydrogel is irreversible formed due to ion diffusion. The second method, called internal gelling, is based on mixing an insoluble source of gelling ions with the alginate solution followed by releasing the gelling ions by lowering the pH value after addition of organic acids or by hydrolyzing lactones (Papajová, Bujdoš, Chorvát, Stach, & Lacík, 2012). When the external gelling method is used for preparation of planar alginate hydrogels, the almost instantly gelation of alginate produces a heterogeneous dispersion of gel lumps. In view of this problem, preparation of planar alginate hydrogels by external gelling requires slow rate of exposure of alginate solution to gelling ions in order to control gelling and hydrogel properties. This issue was tackled by exposing solution of sodium alginate to an aerosolized spray of Ca^{2+} solution (Cathell & Schauer, 2007; Papajová, Bujdoš,

61 Chorvát, Stach, & Lacík, 2012). However, these authors obtained small planar alginate
62 hydrogels. One objective of this research was to develop an ultrasonic atomizing device
63 that allows the preparation of calcium alginate films of larger surface areas, suitable for
64 being used as edible films.
65 On the other hand, although gelation kinetics is altered by the source of calcium, neither
66 the final alginate gel strength nor the resistance to calcium diffusion are modified (Lee,
67 & Rogers, 2012). $CaCl_2$ reaches a gel strength plateau fastest, followed by calcium
68 lactate and calcium gluconate. $CaCl_2$ is the most usual source of calcium when the bitter
69 taste can be masked and a fast throughput is required, while calcium organic salts may
70 have an advantage when the membrane thickness/hardness needs to be manipulated.
71 Calcium gluconolactate, a commonly food additive, is calcium gluconate mixed with
72 calcium lactate. Other objective of the present work was to use calcium gluconolactate
73 as the gelling agent for the formation of dry calcium alginate edible films.
74 In contrast to most gelling polysaccharides, alginate gels have the particular feature of
75 being cold setting and are heat stable. In practice, this means alginate gels can be heat
76 treated without melting. This is the reason why alginates are used in baking creams
77 (Smidsrød & Draget, 2004) as an edible barrier to reduce fat uptake in fried foods
78 (Albert & Mittal, 2002) and as an edible coating that improve the quality of
79 microwaveable chicken nuggets (Albert, Salvador, & Fiszman, 2012). The last objective
80 of this research was to study the physicochemical characteristics of dry calcium alginate
81 films subjected to heat treatment.
82
83 **2. Materials and Methods**
84
85 **2.1. Materials**

Sodium alginate (SA) from brown algae (medium viscosity), calcium lactate hydrate (CLH) and calcium gluconate anhydrous (CGA) were purchased from Sigma-Aldrich (St. Louis, MO, USA). SA had an approximate mannuronic/ guluronic ratio of 1.56, a degree of polymerization range of 400-600, and a molecular weight of 80000-120000. Solid CLH and CGA were mixed at a weight ratio of 4:1. This mixture was called calcium gluconolactate, CG. All other reagents were of analytical grade.

2.2. Preparation of dry alginate films by external gelling method

Solid SA and distilled water were mixed in order to obtain solutions of 0.6% and 0.9% (w/v). The mixtures were magnetically stirred until a homogeneous phase was obtained. Both solutions were degassed by sonication. Following degassing, plastic Petri plates (13.5 cm in diameter) were filled with the different SA solutions assayed (88 g/plate). Then, SA solutions were concentrated by evaporation in an oven (Tecno Dalvo, Santa Fe, Argentina) at 50 °C for 3h. CG solutions were prepared at different concentrations: 0 (for control sample), 1, 2 and 3% (w/v). The concentrations of SA and CG solutions used in this work were selected based on preliminary experiments in which hardness of wet gel measured by a compression test was the critical parameter for selection (Chen & Opara, 2013). In that sense, gels with relative high resistance to deformation without rupture were chosen for the subsequent dried process. The setup used for the formation of alginate hydrogels by external gelling method is shown in Figure 1. The Petri plates were placed on a circular base and covered by a modified plastic dome. The system was driven by an electric engine rotating at 7 rpm. A transparent plastic tube (I.D. 6 mm) connected an ultrasound nebulizer Aspen NU400 (Aspen, Buenos Aires, Argentina) with a diffuser inside the dome. The nebulizer reservoir was filled with the different CG solutions. The aerosol of each gelling solution was introduced into the dome at a flow

rate of 0.3 mL min^{-1} for 20 min. After that, the plates were withdrawn from the system, left to stand at room temperature for 3 h and then put into the oven for 3 h at 50 °C. The dry films were then removed from the Petri dishes and stored in hermetic plastic containers at room temperature. The films used in the different tests were selected based on the lack of physical defects such as cracks, bubbles and holes and on their manageability and flexibility.

2.2.1 Dry film thickness

The thickness of three replicates of each film formulation were measured with an electronic digital disk micrometer (Schwyz®, China) at nine locations on the film to the nearest 1 μm.

2.2.2 Mechanical properties of dry films

Tensile test was carried out using a motorized test frame (Mecmesin Multitest 2.5*d*, Mecmesin, Sterling, VA, USA) equipped with a 100 N digital force gauge. Three sample strips (7 x 60 mm) of each formulation were cut and clamped between tensile grips. The initial distance between grips was 30 mm and the crosshead speed was 0.05 mm s^{-1}. From stress-strain curves, tensile strength (TS) and elongation (E) were determined. TS was calculated by dividing the peak load by the cross sectional area (thickness of film x 7 mm) of the initial film and E was calculated as the percentile of the change in the length of specimen respect to the original distance between the grips (30 mm). TS of the films is a measure of the maximal force per original cross-sectional area that the film could sustain before breaking, and E measures the capacity of the film to extend before breaking (Silva, Bierhalz, & Kieckbusch, 2009).

Mechanical properties, manageability and flexibility were the parameters considered to select the optimum dry film (ODF) to be used in heat treatment studies.

2.3 Heat treatment of dry films

ODF samples were cut into seven rectangular pieces. Each one of the pieces was put between two microscope slides. The end of the microscope slides were then clamped together using bulldog clips. The samples were heated (ODFH) in a forced oven at 180 °C (Industrias Brafh, Rosario, Argentina). To study the effect of heating, each piece was withdrawn at different heating times (0, 4, 8, 12, 16, 20 and 24 min). This experiment was repeated three times.

2.3.1 Thickness and mechanical properties of heat treated samples

The thickness and mechanical properties of ODFH samples were measured in accordance with section 2.2.1 and section 2.2.2.

2.3.2 Optical properties

2.3.2.1 Opacity

Opacity of ODFH samples was evaluated according the method of Siripatrawan and Harte (2010) with modifications. ODFH samples were cut into rectangular pieces (10 x 30 mm), heat treated in agreement with section 2.3 and placed on the internal side of a spectrophotometer cell (Jasco V-550, Tokyo, Japan). Light absorbance of the film samples was measured at 600 nm and the opacity was calculated using the following equation:

160 Opacity = Abs_{600} / l (1)

161

162 where Abs_{600} is the value of absorbance at 600 nm ant l is the film thickness in mm.

163

164 **2.3.2.2 Color measurements**

165 ODFH samples were used to obtain the digital images. A wooden box according to the
166 design described in Mendoza and Aguilera (2004), with some modifications, was used.
167 Samples were illuminated using four fluorescent lamps (Osram, Biolux, Natural
168 Daylight, 18W/965, Munich, Germany) with a color temperature of 6500 K (*D65*,
169 standard light source commonly used in food research) and a color-rendering index Ra
170 of 95%. Additionally, electronic ballast and an acrylic light diffuser ensured uniform
171 illumination system. Samples were photographed employing a digital camera (Nikon P
172 7100, Nikon, Jakarta, Indonesia) on a matte white background using the following
173 camera settings: manual mode with lens aperture at f = 8 and time of exposition 1/200,
174 no flash, ISO sensibility 400, maximum resolution (3648 x 2736 pixels), and storage in
175 RAW format.
176 An IT8 calibration card (Wolf Faust, Germany) was photographed under the same
177 conditions than heat treated films and was used to obtain the International Colour
178 Consortium (ICC) profile employing the Lprof software (Free Software Foundation,
179 Inc., Boston, MA, USA). This profile was applied to sample images using Photoshop
180 (Adobe Systems, Inc., USA). *L*, *a*, and *b* average values (considering the whole sample)
181 were obtained from histogram window and then were converted to *L** (lightness), *a**
182 (red-green), and *b** (yellow-blue) following the work of Yam and Papadakis (2004).
183 Total colour differences (ΔE) were calculated as follows:

184

$$\Delta E = \sqrt{\Delta L^2 + \Delta a^2 + \Delta b^2} \quad (2)$$

$$\Delta L = L^* - L_0^* \quad (3)$$

$$\Delta a = a^* - a_0^* \quad (4)$$

$$\Delta b = b^* - b_0^* \quad (5)$$

where L_0^*, a_0^* and b_0^* are the standard values of the standard white plate and L^*, a^* and b^* are the measured values of the sample.

2.3.3 Differential scanning calorimetry (DSC)

Thermal properties of ODF, SA, CLH and CGA were measured using a differential scanning calorimeter (DSC-60, Shimadzu, Kyoto, Japan). Aliquots of approximately 10 mg of dried samples were placed into aluminum pans, sealed and scanned over the range 30-350 °C with a heating rate of 10° C min^{-1}. The empty aluminum pan was used as a reference. Each sample was run in duplicate.

2.3.4 Fourier transform infrared (FTIR) spectroscopy

The spectra of ODF and ODFH samples were determined using FTIR with an IR-Prestige-21 spectrophotometer (Shimadzu, Kyoto, Japan) under attenuated total reflectance (ATR) mode. The spectra were recorded in absorbance mode from 600 to 4000 cm^{-1} using 20 scans at 4 cm^{-1} resolution.

209 **2.3.5 Scanning electron microscopy (SEM)**

210 In order to study the influence of heat treatment on ODFH microstructure, SEM
211 experiments were carried out. Film samples were cryo-fractured by immersion in liquid
212 nitrogen and mounted on bronze stubs perpendicularly to their surface. The portions
213 were coated with gold during 15 min at 70-80 mTorr. Micrographs of films cross-
214 section were taken with a scanning electron microscope (AMR 1000, Leitz, Wetzlar,
215 Germany) using an accelerating voltage of 20 kV. Magnification of 500 was used in this
216 work.

217

218 **2.4 Statistical analysis**

219 Statistical analysis was performed using Statgraphics Plus for Windows (Manugistics
220 Inc, Rockville, MA, USA). Analysis of variance (ANOVA) was used and when the
221 effect of the factors was significant ($p < 0.05$), the test of multiple ranks honestly
222 significant difference (HSD) of Tukey was applied (95% of confidence level).

223

224 **3. Results and Discussion**

225

226 **3.1. Appearance and thickness of the films**

227 Calcium alginate films obtained by the methodology described in Section 2.2. were
228 visually homogeneous without brittle areas or bubbles. In addition, the films were easily
229 manageable and flexible.

230 Figure 2 shows the thickness of the films prepared from SA solutions of 0.6 and 0.9%
231 (w/v) in presence of different CG concentrations in the nebulizer reservoir. Film
232 thickness increased as the concentration of SA increased for all the CG concentrations
233 assayed ($p < 0.05$), Figure 2. As can also be seen in this Figure, the presence of CG

234 increased film thickness at both SA concentrations assayed ($p < 0.05$). However, no
235 significant difference was found between CG concentrations at each SA concentration
236 studied ($p < 0.05$). These results were similar to those reported previously by Rhim
237 (2004) who prepared calcium alginate films by direct addition of $CaCl_2$ into sodium
238 alginate solutions (mixing films).
239
240 **3.2 Mechanical properties**
241 Tensile strength of films prepared from SA solutions of 0.6 and 0.9% (w/v) in presence
242 of different CG concentrations in the nebulizer reservoir is shown in Figure 3. Calcium
243 alginate films were strong as indicated by high values of TS. TS of the films
244 significantly increased as the concentration of SA increased for all the CG
245 concentrations in the nebulizer reservoir assayed ($p < 0.05$). On the other hand, as CG
246 concentration increased first a strengthening and then a weakening of films was
247 observed for both SA concentrations studied ($p < 0.05$). TS increased up to 2% CG
248 concentration while beyond this value a decrease in this mechanical property was
249 observed. A similar pattern was observed by Cuadros, Skurtys and Aguilera (2012) for
250 calcium alginate fibers produced with a microfluidic device. These authors suggested
251 that the "egg-box" model used to describe ionotropic gelation of alginate only partly
252 explains the relation with microstructural and mechanical properties of the gelled
253 material and proposed that the decrease in gel strength that was observed after the
254 maximum was achieved, was due to the reversion of the system to the formation of
255 dimers with no association between them.
256 Figure 4 shows that E of the films significantly increased as the concentration of SA
257 increased for all the CG concentrations ($p < 0.05$). On the other hand, E significantly
258 increased when 1% CG concentration was used, while beyond 2% a decrease in this

mechanical property was observed. E is related to the ability of a material to resist changes of shape without cracking. The E values obtained in the present work for calcium alginate films were similar to those reported by Rhim (2004).

In view of the results of mechanical properties, manageability and flexibility, calcium alginate films obtained using 0.9% SA concentration and 2% CG concentration in the nebulizer reservoir were selected as the optimum dry film (ODF) to be used in heat treatment studies.

3.3 Characterization of ODFH samples

While the visual aspect of ODFH samples is shown in Figure 5, Table 1 presents their thickness and optical parameters. Thickness of ODFH samples dramatically decreased up to 8 min of heat treatment, possibly due to a dehydration process.

Opacity is an established measurement of the transparency of a film. A higher value of opacity means a lesser transparency (Pereda, Amica, Rácz, & Marcovich, 2011). The tendency of opacity to increase with the length of heating may be attributed to two factors: an intense color development and the decrease in the thickness of the film (Equation 1). The color properties of ODFH samples summarized in Table 1 reinforce this suggestion. ODFH samples changed their appearance from transparent yellow to opaque yellow ochre in function of heating time. In that sense, after 24 min of heat treatment, ΔE increased approximately 14 times. This change was principally promoted by redness (a^*), while yellowness (b^*) and changes in lightness (L^*) played a minor role. These changes in color parameters can be assigned to chemical degradation of the components of the system.

Mechanical properties of ODFH samples are presented in Figure 6 and Figure 7. Figure 6 shows that heat treatment for 4 min and 8 min at 180 °C produced a significant

284 increase in TS values compared to the sample without any treatment. However, heating
285 for longer times promoted a decrease in TS of ODFH samples. Despite this decrease in
286 TS, the values obtained in this range remained relatively high (Rhim, 2004). On the
287 other hand, E decreased gradually with the intensity of heat treatment (Figure 7). In that
288 sense, E reduced approximately 3 times in comparison to the sample without treatment
289 after 24 min of heating. As a result of these changes, an increase in the brittleness of
290 ODFH with the severity of heat treatment was observed. It can be considered that
291 dehydration process was a determining factor in mechanical properties modifications.
292 Figure 8 shows DSC thermograms of the different samples assayed in this work. ODF
293 samples presented an endothermic peak at 99 °C that corresponds to dehydration of the
294 cross-linked gel matrix (alginate-calcium cation) (Taha, Nasser, Ardakani, & Al Khatib,
295 2008). The exothermic peaks observed at temperatures between 175 and 275 °C result
296 from degradation of alginate due to dehydration and depolymerisation of the protonated
297 carboxylic groups and oxidation reactions of the macromolecule (Sarmento, Ferreira,
298 Veiga, & Ribeiro, 2006). SA thermograms were consistent with those reported
299 previously (Al-Remawi, 2012). In that sense, SA presented similar thermogram patterns
300 as ODF samples, with an endothermic band due to dehydration and a dehydration-
301 degradation band at higher temperatures. CLH showed a dehydration peak at 100 °C
302 although did not show degradation peaks at temperatures below 300 °C (Sakata,
303 Shiraushi, & Otsuka, 2005). In contrast, CGA only showed a degradation peak near 250
304 °C. These last results strengthen the hypothesis that the observed changes in thickness
305 and mechanical properties could be assigned to dehydration of the alginate-calcium ion
306 matrix, while early stages of degradation of alginate were the cause of color changes in
307 ODFH samples (Figure 5).

FTIR spectra of ODF samples (Figure 9) showed characteristics peaks of alginate: hydroxyl group at ≈ 3220 cm^{-1} (stretching) and carboxylate peaks at ≈ 1590 and 1410 cm^{-1} (asymmetric and symmetric stretching) (Campañone, Bruno, & Martino, 2014). The presence of large amount of water in alginate solutions resulted in the saturation of signal for O-H stretching band around 3000-3600 cm^{-1} wavenumber (Xiao, Gu, & Tan, 2014). However, the drying process applied in this work to calcium alginate gels drastically reduced the intensity of this band. The further decrease in the intensity of this band promoted by heat treatment (ODFH samples) may be explained by the release of additional water molecules retained in the film matrix. Figure 9 also shows that as the heat treatment progressed, the intensity of the band around 1590 and 1410 cm^{-1} increased. Similar phenomenon has been reported by Xiao et al. (2014) for the drying process of sodium alginate films. These authors attributed this behavior to the evaporation of water.

SEM micrographs of fractured surface revealed that heat treatment affected the internal microstructure of films, Figure 10. ODF showed a more homogeneous structure when compared with ODFH sample. Cross-section of ODFH heated for 24 min at 180 °C showed a reduced thickness and a laminar structure produced by strong dehydration. This heterogeneous matrix of ODFH is an indicator of the loss of structural integrity, and consequently higher mechanical brittleness.

4. Conclusions

Dry calcium alginate films of adequate size and mechanical properties, suitable to be used as edible films, were obtained using a novel device in which a sodium alginate solution was nebulised with a calcium gluconolactate solution as gelling agent. The dry films obtained were then subjected to heat treatment at 180 °C for different times and

physicochemical characteristics of the resultant products were analyzed. Heat treatment produced thickness reduction, a yellow ochre color development and an increase in the brittleness of the dry films. DSC, FTIR and SEM studies suggested that the changes observed may be attributed to further dehydration of dry films and to the first steps of thermal degradation of alginate macromolecules. These studies point to a potential application of these heat-treated films as enhancers of crisp texture and optical properties of foodstuffs.

Acknowledgements

This work was supported by grants from Universidad Nacional de Rosario (UNR), Consejo Nacional de Investigaciones Científicas y Técnicas (CONICET), Secretaría de Estado de Ciencia, Tecnología e Innovación de la Provincia de Santa Fe (SECTeI) and Agencia Nacional de Promoción Científica y Tecnológica de la República Argentina (ANPCyT).

References

Al-Remawi, M. (2012). Sucrose as a crosslinking modifier for the preparation of calcium alginate films via external gelation. *Journal of Applied Sciences*, 12(8), 727-735.

Albert, S., & Mittal, G.S. (2002). Comparative evaluation of edible coatings to reduce fat uptake in a deep-fried cereal product. *Food Research International*, 35(5), 445-458.

Albert, A., Salvador, A., & Fiszman, S.M. (2012). A film of alginate plus salt as an edible susceptor in microwaveable food. *Food Hydrocolloids*, 27(2), 421-426.

Campañone, L., Bruno, E., & Martino, M. (2014). Effect of microwave treatment on metal-alginate beads. *Journal of Food Engineering*, 135, 26-30

Cathell, C.L., & Schauer, C.L. (2007). Structurally colored thin films of Ca^{2+}-cross-linked alginate. *Biomacromolecules*, 8(1), 33-41.

Chen, L., & Opara, U.L. (2013). Texture measurements approaches in fresh and processed foods – A review. *Food Research International*, 51(2), 823-835.

Cuadros, T.R., Skurtys, O., & Aguilera, J.M. (2012). Mechanical properties of calcium alginate fibers produced with a microfluidic device. *Carbohydrate Polymers*, 89(4), 1198-1206.

Draget, K.I. (2000). Alginates. In G.O. Phillips, & P.A. Williams (Eds.), Handbook of hydrocolloids (pp. 379–395). Boca Raton: CRC Press.

Grant, G.T., Morris, E.R., Rees, D.A., & Smith, P.J.C. (1973). Biological interactions between polysaccharides and divalent cations: The egg-box model. *FEBS Letters*, 32(1), 195-198.

Lee, P., & Rogers, M.A. (2012). Effect of calcium source and exposure-time on basic caviar spherification using sodium alginate. *International Journal of gastronomy and Food Science*, 1(2), 96-100.

383 Mendoza, F., & Aguilera, J. M. (2004). Application of image analysis for classification
384 of ripening bananas. *Journal of Food Science*, 69(9), 474-477.
385
386 Papajová, E., Bujdoš, M., Chorvát, D, Stach, M, & Lacík, I. (2012). Method for
387 preparation of planar alginate hydrogels by external gelling using an aerosol of gelling
388 solution. *Carbohydrate Polymers*, 90(1), 472-482.
389
390 Pereda, M., Amica, G., Rácz, I., & Marcovich, N.E. (2011). Structure and properties of
391 nanocomposite films based on sodium caseinate and nanocellulose. *Journal of Food*
392 *Engineering*, 103(1), 76-83.
393
394 Rhim, J.W. (2004). Physical and mechanical properties of water resistant sodium
395 alginate films. *Lebensmittel-Wissenschaft und-Technologie*, 37(3), 323-330.
396
397 Sakata, Y., Shiraishi. S., & Otsuka, M. (2005). Characterization of dehydration and
398 hydration behavior of calcium lactate pentahydrate and its anhydrate, *Colloids and*
399 *Surfaces B: Biointerfaces*, 46(3), 135-141.
400
401 Sarmento, B., Ferreira, D., Veiga, F., & Ribeiro, A. (2006). Characterization of insulin-
402 loaded alginate nanoparticles produced by ionotropic pre-gelation through DSC and
403 FTIR studies. *Carbohydrate Polymers*, 66(1), 1-7.
404
405 Silva, M.A., Bierhalz, A.C.K., & Kieckbusch, T.G. (2009). Alginate and pectin
406 composite films crosslinked with Ca^{2+} ions: effects of the plasticizer concentration.
407 *Carbohydrate Polymers* 77(4), 736-742.

Siripatrawan, U., & Harte, B.R. (2010). Physical properties and antioxidant activity of an active film from chitosan incorporated with green tea extract. *Food Hydrocolloids,* 24, 770-775.

Smidsrød & Draget, K.I. (2004). Alginate gelation technologies. In E. Dickinson, & B. Bergenstål (Eds.), Food Colloids. Protein, lipids and polysaccharides (pp. 279–293). Abington Hall: Woodhead Publishing Ltd.

Taha, M.O., Nasser, W., Ardakani, A., & Al Khatib, H.S. (2008). Sodium lauryl sulfate impedes drug release from zink-crosslinked alginate beads: Switching from enteric coating release into biphasic profiles. *International Journal of Pharmaceutics*, 350(1-2), 291-300.

Xiao, Q., Gu, X, & Tan, S. (2014). Drying process of sodium alginate films studied by two dimensional correlation ATR-FTIR spectroscopy. *Food Chemistry*, 164, 179-184

Yam, K. L., & Papadakis, S. E. (2004). A simple digital imaging method for measuring and analyzing color of food surfaces. *Journal of Food Engineering*, 61, 137–142.

Figure captions

Figure 1. Experimental setup for formation of planar alginate hydrogels by external gelling method.

Figure 2. Thickness of films prepared with different sodium alginate concentrations in presence of different calcium gluconolactate concentrations in the nebulizer reservoir. Each value is the mean of three replicates. Error bars indicate standard deviations. Different letters above columns indicate significant differences ($p < 0.05$).

Figure 3. Tensile strength of films prepared with different sodium alginate concentrations in presence of different calcium gluconolactate concentrations in the nebulizer reservoir. Each value is the mean of three replicates. Error bars indicate standard deviations. Lower case letters indicate significant differences between sodium alginate concentrations for each calcium gluconolactate solution assayed ($p < 0.05$). Upper case letters indicate significant differences among calcium gluconolactate concentrations for each sodium alginate solution used ($p < 0.05$).

Figure 4. Elongation of films prepared with different sodium alginate concentrations in presence of different calcium gluconolactate concentrations in the nebulizer reservoir. Each value is the mean of three replicates. Error bars indicate standard deviations. Lower case letters indicates significant differences between sodium alginate concentrations for each calcium gluconolactate solution assayed ($p < 0.05$). Upper case letters indicates significant differences among calcium gluconolactate concentrations for each sodium alginate solution used ($p < 0.05$).

Figure 5. Photographs of heated optimum dry film samples.

Figure 6. Tensile strength of heated optimum dry film samples. Each value is the mean of three replicates. Error bars indicate standard deviations. Different letters above columns indicate significant differences ($p < 0.05$).

Figure 7. Elongation of heated optimum dry film samples. Each value is the mean of three replicates. Error bars indicate standard deviations. Different letters above columns indicate significant differences ($p < 0.05$).

Figure 8. Differential scanning calorimetry thermograms of (a) optimum dry film, (b) sodium alginate, (c) calcium lactate hydrate and (d) calcium gluconate anhydrous samples.

Figure 9. Fourier transform infrared spectra of optimum dry film: (──) and optimum dry film heated for 24 min at 180 °C: (─ • ─).

Figure 10. Scanning electron microscopy micrographs of (a) optimum dry film and (b) optimum dry film heated for 24 min at 180 °C.

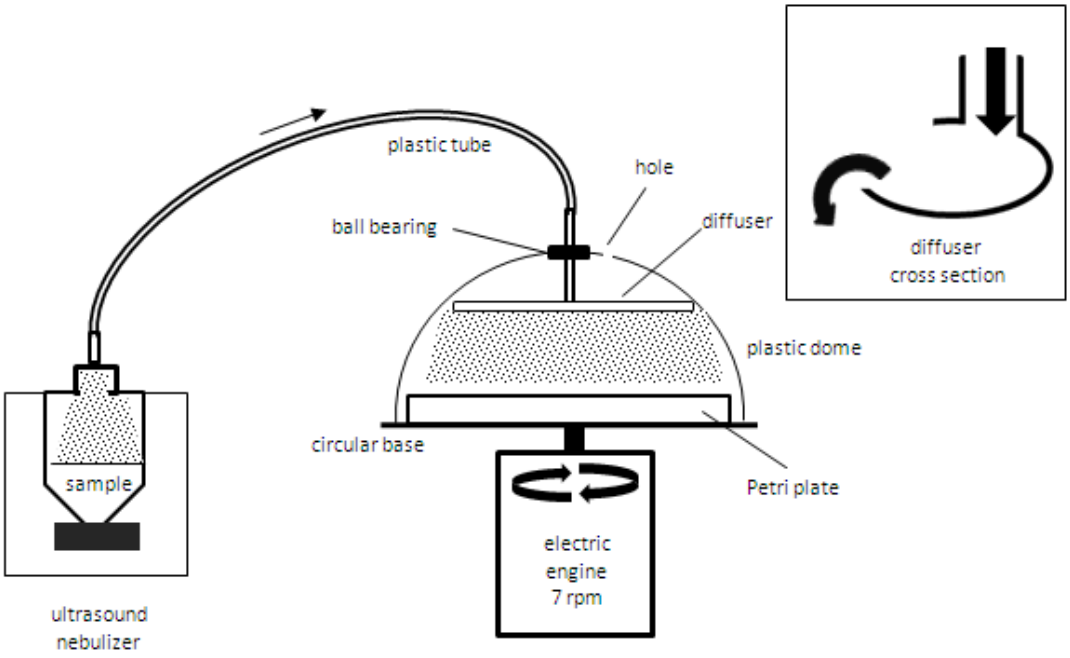
plastic tube
hole
ball bearing
diffuser
diffuser
cross section
plastic dome
circular base
Petri plate
sample
electric
engine
7 rpm
ultrasound
nebulizer

Figure 1

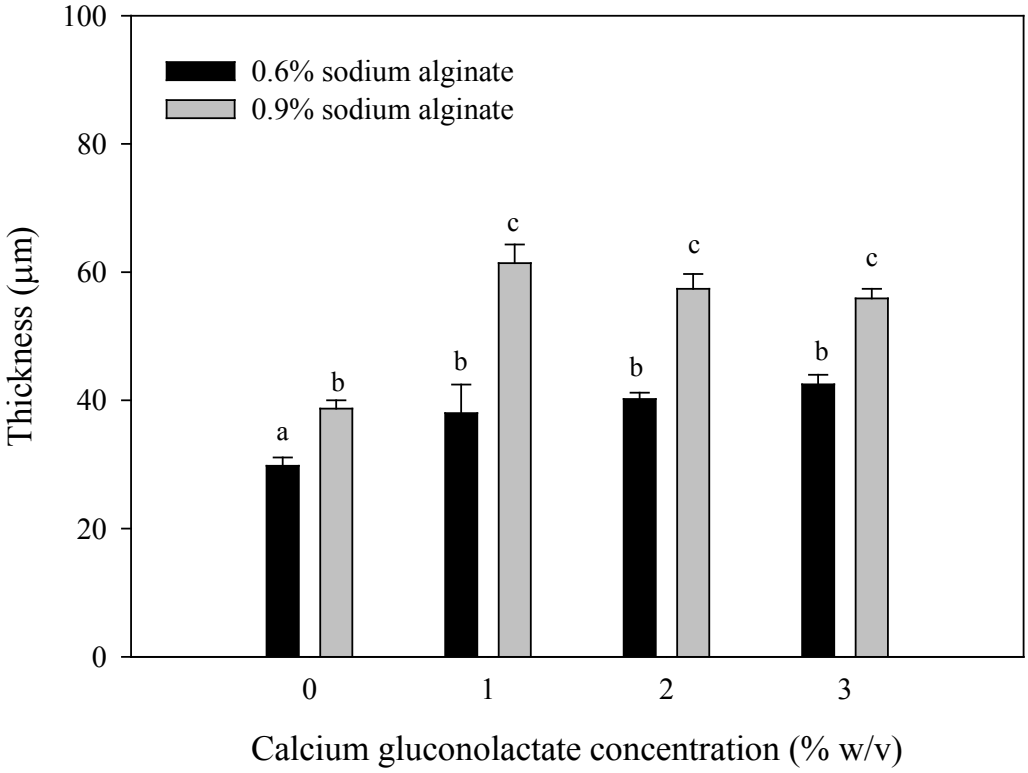
100
80
60
40
20
0
Thickness (µm)
0.6% sodium alginate
0.9% sodium alginate
a
b
b
c
b
c
b
c
0
1
2
3
Calcium gluconolactate concentration (% w/v)

Figure 2

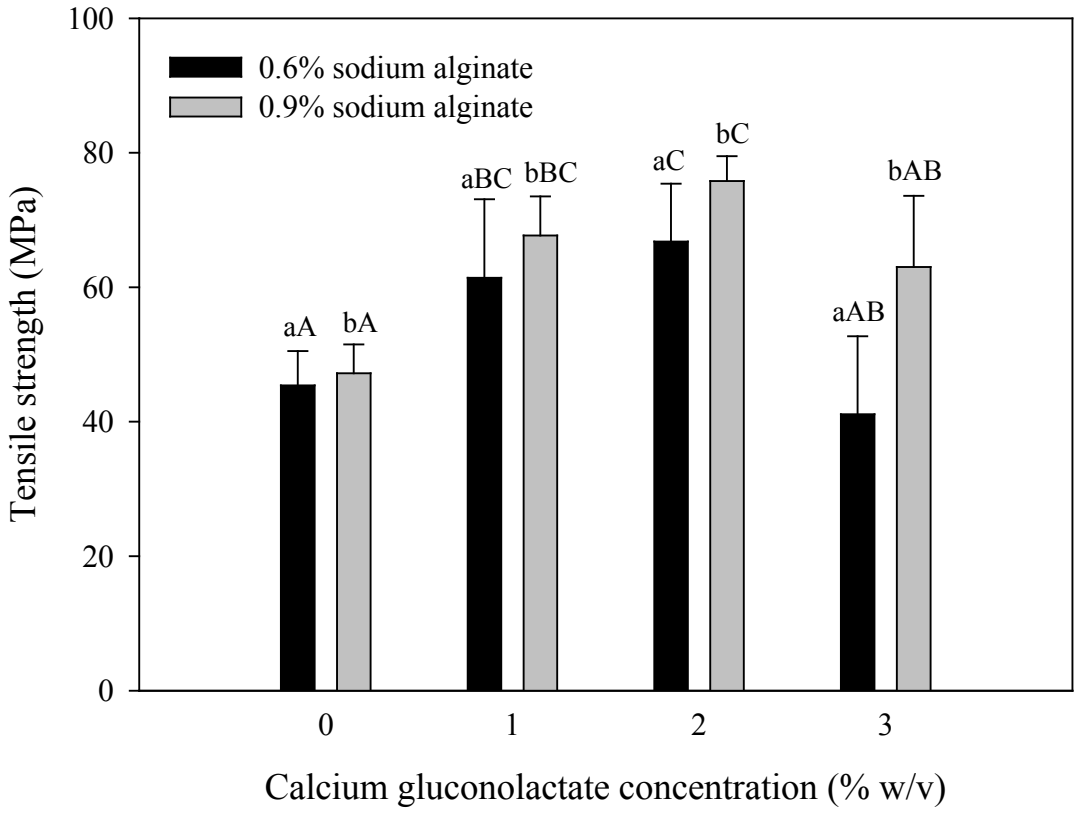
100
80
60
40
20
0
Tensile strength (MPa)
0.6% sodium alginate
0.9% sodium alginate
aA
bA
aBC
bBC
aC
bC
aAB
bAB
0
1
2
3
Calcium gluconolactate concentration (% w/v)

Figure 3

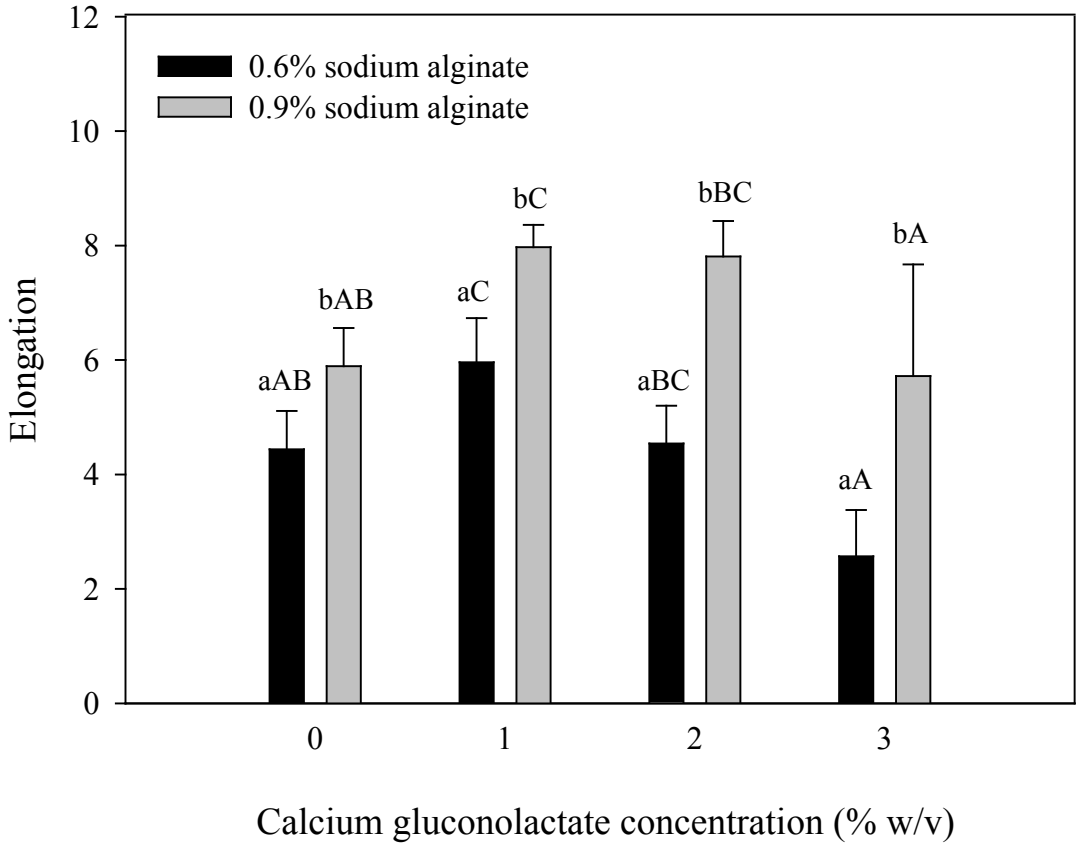
12
10
8
6
4
2
0
Elongation
0.6% sodium alginate
0.9% sodium alginate
aAB
bAB
aC
bC
aBC
bBC
aA
bA
0
1
2
3
Calcium gluconolactate concentration (% w/v)

Figure 4

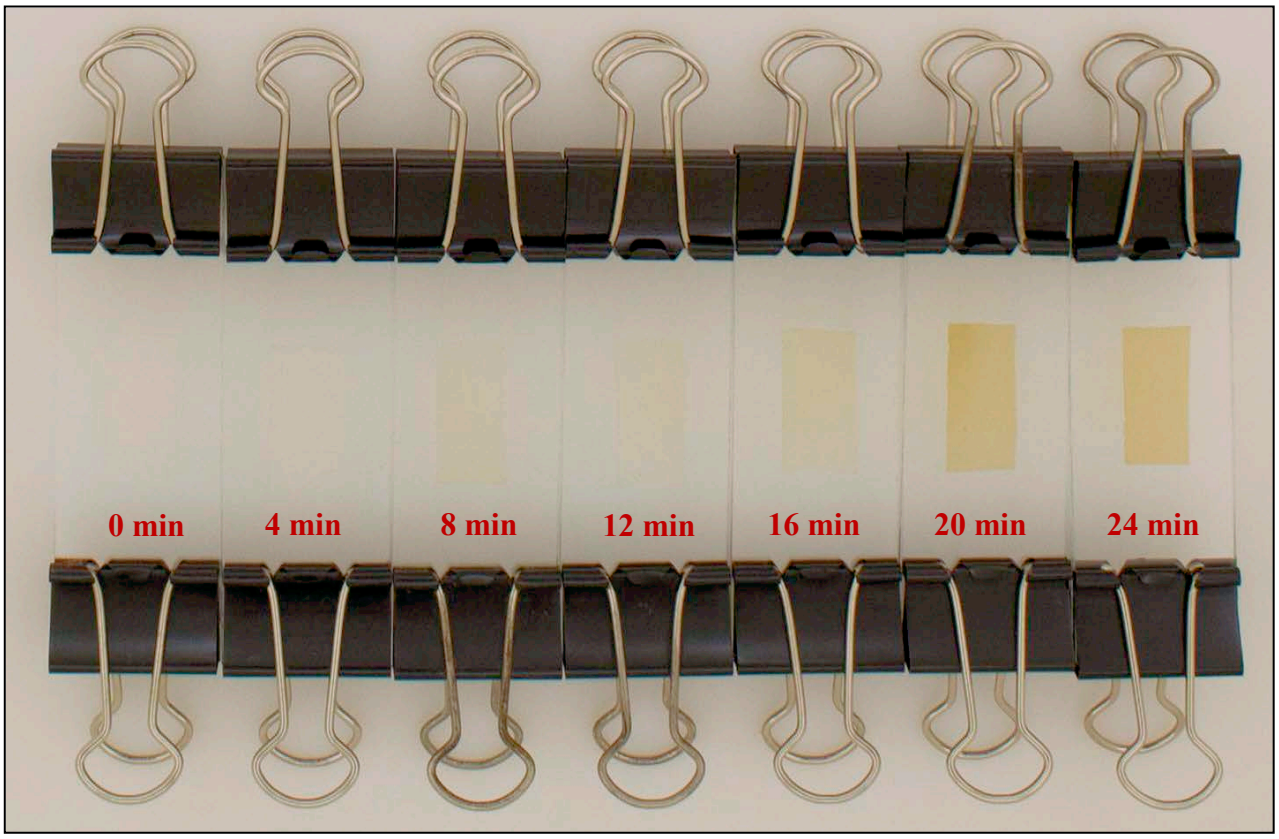

Figure 5

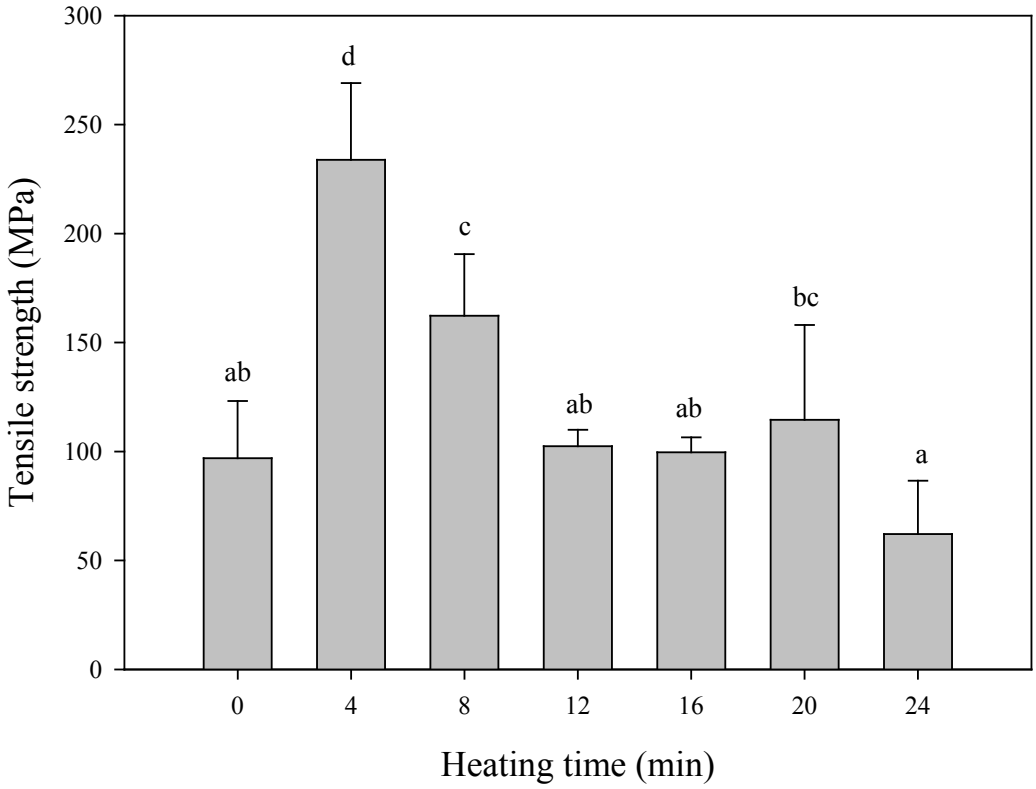
Tensile strength (MPa)
300
250
200
150
100
50
0
d
c
bc
ab
ab
ab
a
0
4
8
12
16
20
24
Heating time (min)

Figure 6

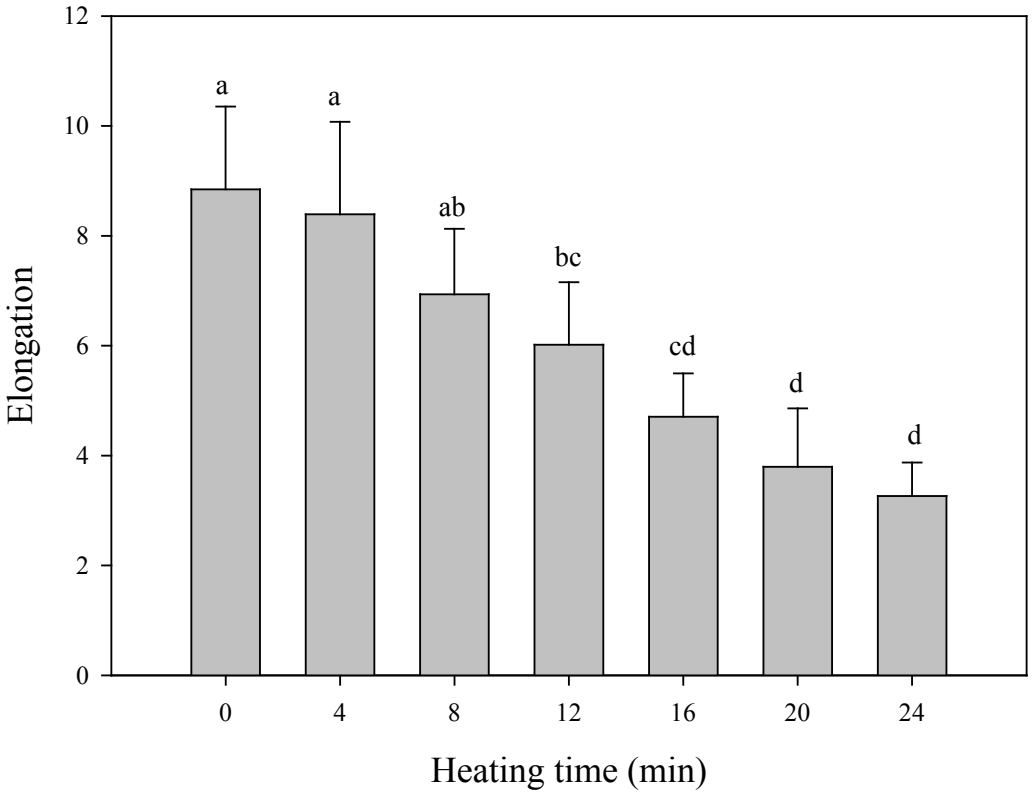
12
10
8
6
4
2
0
Elongation
a
a
ab
bc
cd
d
d
0
4
8
12
16
20
24
Heating time (min)

Figure 7

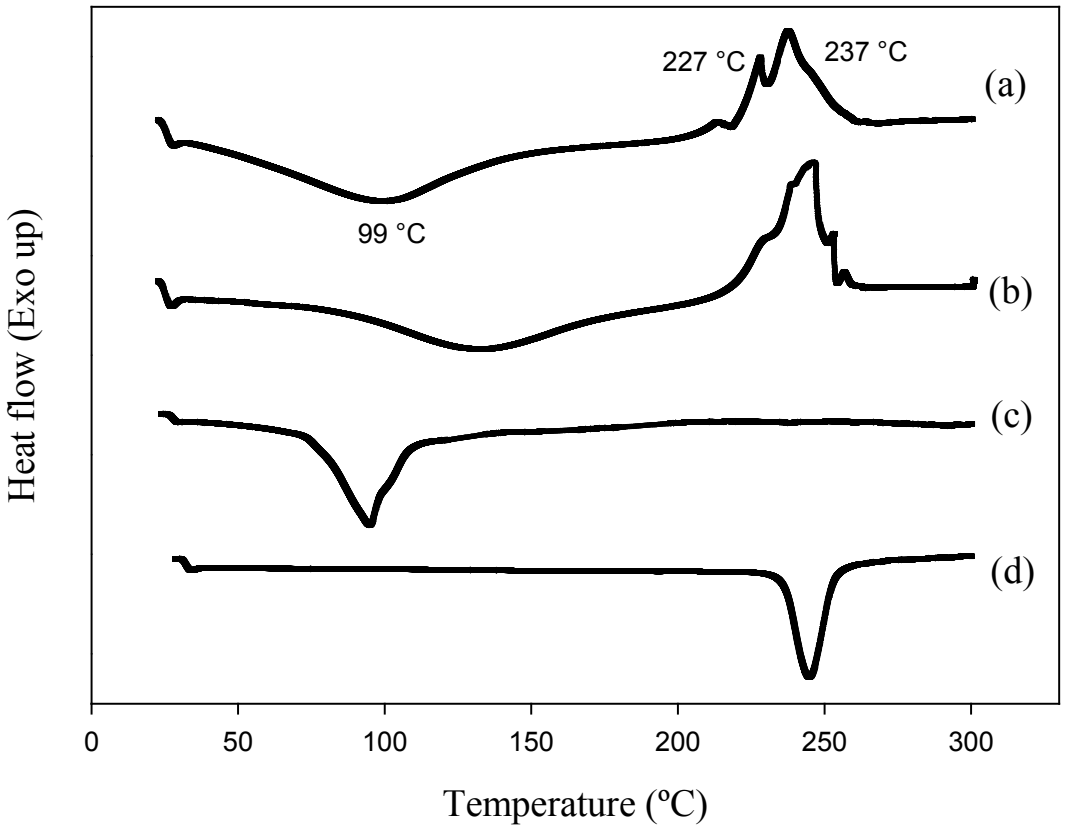
227 °C
237 °C
(a)
99 °C
(b)
(c)
(d)
Heat flow (Exo up)
0
50
100
150
200
250
300
Temperature (ºC)

Figure 8

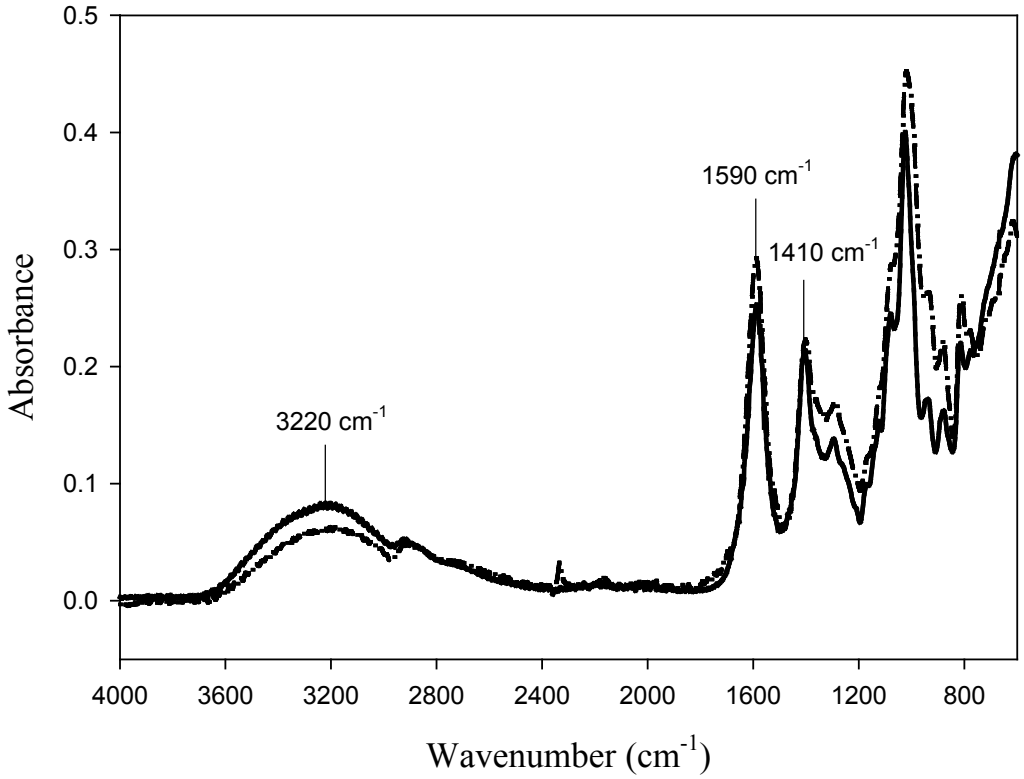
0.5
0.4
0.3
0.2
0.1
0.0
Absorbance
1590 cm-1
1410 cm-1
3220 cm-1
4000
3600
3200
2800
2400
2000
1600
1200
800
Wavenumber (cm-1)

Figure 9